

Nickel-Catalyzed Domino Cross-Electrophile Coupling Dicarbofunctionalization Reaction to Afford Vinylcyclopropanes

Kirsten A. Hewitt^{†‡}, Pei-Pei Xie^{‡‡}, Taylor A. Thane[†], Nadia Hirbawi[†], Shuo-Qing Zhang[‡], Alissa C. Matus[†], Erika L. Lucas[†], Xin Hong^{*‡}, Elizabeth R. Jarvo^{*†}

[†]Department of Chemistry, University of California, Irvine, California, 92697

[‡]Center of Chemistry for Frontier Technologies, Department of Chemistry, Zhejiang University, Hangzhou, 310027, China

ABSTRACT: We have established a nickel-catalyzed domino reaction that harnesses sulfonamide, alkyl chloride, and alkyne functionalities in a multistep sequence to afford vinylcyclopropanes bearing tetrasubstituted olefins. Starting materials are prepared by iron-promoted aza-Prins reactions of ynals. This method provides rapid synthetic access to valuable building blocks with applications in medicinal chemistry. Experimental and computational results support initiation of the catalytic cycle by oxidative addition of the propargylic sulfonamide and a key ambiphilic allenynickel intermediate leads to a bifurcated reaction pathway that generates olefin isomers

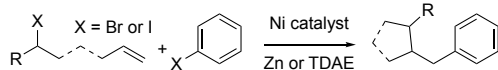
Domino reactions provide powerful strategies to build molecular complexity by forging multiple C–C bonds and stereogenic centers in a single reaction flask.¹ Development of these reactions typically builds on mechanistic understanding of discrete elementary steps, established in simpler transformations. Incorporation of cross-electrophile coupling (XEC) reactions into domino sequences is in its early stages.² Recent efforts have established nickel-catalyzed conjunctive XEC reactions where two organohalides are utilized to functionalize an alkene in the presence of a reducing agent (Scheme 1a).^{3,4,5,6} These reactions intersect traditional XEC reaction mechanisms because they involve two oxidative addition events and, frequently, alkyl radical intermediates.⁷ *Domino methods that combine XEC reactions with additional C–C bond-forming reactions have not been reported.*

We sought to develop a domino reaction building on our nickel-catalyzed XEC reactions of ethers and sulfonamides (Scheme 1b).^{8,9} In contrast with other XEC mechanisms, these reactions avoid radical intermediates, initiate with a polar oxidative addition of an activated C–O or C–N bond,¹⁰ and cascade forward via an intramolecular S_N2-type reaction. Based on the calculated reaction coordinate, catalyst turnover by reduction of Ni(II) to Ni(0) with formation of ethane is rate-determining. Therefore, this catalytic cycle presents an opportunity to develop new domino transformations by inserting elementary steps known for Ni(II) intermediates.^{11,12,13} In this manuscript, we disclose a nickel-catalyzed domino reaction that combines intramolecular XEC and dicarbofunctionalization reactions to produce substituted vinylcyclopropanes (Scheme 1c). This

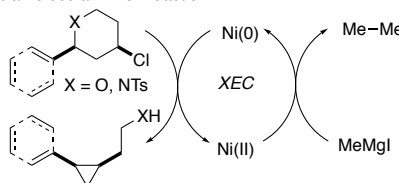
multicomponent transformation produces three new carbon–carbon bonds and a strained ring. The cyclopropane moiety is produced with high stereochemical fidelity. In addition, we provide experimental and computational evidence that the mechanism involves a single oxidative addition, an intramolecular S_N2-type reaction and a single reductive elimination. All elementary steps are stereospecific; product isomers result from divergent pathways from a key allenynickel intermediate.

Scheme 1. Nickel-Catalyzed Domino XEC Reactions

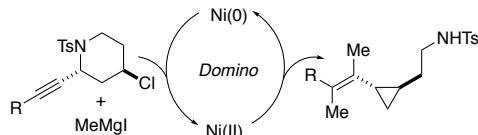
a. Conjunctive XEC reactions



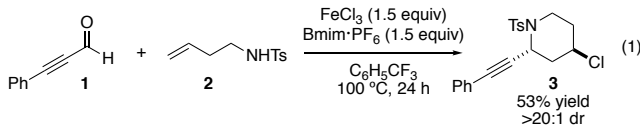
b. Intramolecular XEC Reaction



c. This work: XEC-Dicarbofunctionalization Domino Reaction



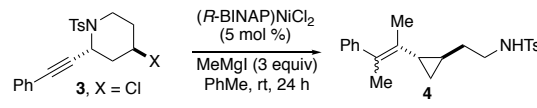
At the outset, we recognized that a critical component of our approach would be the rapid and efficient synthesis of the requisite starting materials. We envisioned that an aza-Prins reaction could generate 4-halo-2-alkynyl piperidines directly from ynals.¹⁴ Unfortunately, there were no Prins or aza-Prins reactions of simple ynals in the literature. The closest precedence was a cobalt-mediated reaction, where the cobalt complex serves to mask the alkyne to produce protected 2-alkynyl tetrahydropyrans.¹⁵ We were encouraged, however, by iron-promoted aza-Prins reactions of enals for synthesis of 2-vinyl piperidines.¹⁶ We applied similar conditions for the aza-Prins reaction of ynals (eq 1). Gratifyingly, this reaction afforded the desired 2-alkynyl-4-chloropiperidine in 53% yield and as a single diastereomer. As expected, the *trans* diastereomer was preferred due to minimization of A(1,3)-strain.¹⁷ This transformation proved to be robust across a range of aryl- and alkyl-substituted ynals (*vide infra*).¹⁸



We investigated the feasibility of the proposed domino reaction employing *N*-tosyl piperidine **3**.¹⁹ We began with the previously developed conditions for the XEC reaction of aryl and vinyl sulfonamides with (*R*-BINAP) NiCl_2 as the precatalyst (Table 1, entry 1).^{8c,20} We evaluated two halide leaving groups, and the chloride produced the functionalized cyclopropane in greater yield as compared to the fluoride (entries 1 and 2).²¹ We determined by NMR analysis that the cyclopropane moiety is exclusively produced as the *trans* configuration while the olefin is generated as a mixture of (*E*)- and (*Z*)-alkene isomers.¹⁸ In an attempt to improve diastereoselectivity, we cooled the reaction to 0 °C, however, no product was formed and 98% starting material was recovered (entry 3). Previously, our laboratory has found that Lewis acidic MgI_2 can accelerate the rate of oxidative addition of sluggish electrophiles,^{9,22} however, the yield of the domino reaction did not improve with the addition of one equivalent of MgI_2 (entry 4). When the number of equivalents of the Grignard reagent was lowered, the yield improved (entries 5 and 6). Next, we evaluated alternative precatalysts. The commercially available Jamison catalyst, *cis*-(*R*-BINAP) $\text{Ni}(\text{o-tolyl})\text{Cl}$, afforded similar yield and *E:Z* ratios (entry 7).^{20a} $\text{Ni}(\text{cod})_2$ and racemic BINAP provided decreased yield, consistent with our prior observation that cod inhibits

XEC reactions of sulfonamides.^{8c} Other precursors also afforded modest yields (entries 9 and 10).²³ Finally, we observed that the nickel catalyst was essential for the domino reaction to take place. In the absence of catalyst, simple propargylic displacement by the Grignard reagent occurred in 15% yield (entry 11).^{24,25} We hypothesized that allenylcopper intermediates could potentially engage in an XEC reaction.^{26,27,28} However, in preliminary investigations, when the nickel precatalyst was replaced with a copper salt no reaction was observed (entry 12). Therefore, we concluded that the optimal domino conditions employ a nickel(II) precatalyst, BINAP as the ligand, and two equivalents of methylmagnesium iodide.

Table 1. Optimization of Nickel-Catalyzed Domino Reaction



Entry	Deviation from Standard Conditions	Yield (%) ^a	<i>E:Z</i>
1	none	61	1.5 : 1
2	X = F	51	1.1 : 1
3	0 °C instead of rt	<5	—
4	1.0 equiv of MgI_2 added	61	1.7 : 1
5	2.5 equiv MeMgI	68	1.5 : 1
6	2 equiv MeMgI	72 (71) ^b	1.7 : 1
<i>(R</i> -BINAP) NiCl_2 replaced with 5 mol % of:			
7	<i>cis</i> -(<i>R</i> -BINAP) $\text{Ni}(\text{o-tolyl})\text{Cl}$	74	1.2 : 1
8	$\text{Ni}(\text{cod})_2$, <i>rac</i> -BINAP	30	1 : 2
9 ^c	$\text{Ni}(\text{cod})(\text{DQ})$, <i>rac</i> -BINAP	42	1 : 1.2
10 ^c	$\text{Ni}(\text{acac})_2$, <i>rac</i> -BINAP	52	1 : 1.6
11	No Nickel Catalyst	<5	—
12 ^d	$\text{Cu}(\text{CH}_3\text{CN})_4\text{OTf}$	<5	—

^aDetermined by ¹H NMR based on comparison to PhTMS as an internal standard. ^bIsolated yield. ^c2 equiv of methylmagnesium iodide. ^dPhMe replaced with DCM.

To determine the functional group compatibility of this reaction, a series of experiments to probe the reaction robustness were performed (Figure 1).²⁹ Since this transformation employs a nucleophilic Grignard reagent, we first targeted functional groups that are sensitive to methylmagnesium iodide. We began by evaluating acidic moieties. Phenol, thiophenol, and aniline were all tolerated under the reaction conditions, given excess Grignard reagent to account for proton transfer, allowing for moderate to good yields of cyclopropane **4**. We were also pleased to note that a silyl ether was well tolerated. Nitrobenzene inhibited the nickel catalyst and poor yields of cyclopropane **4** were observed. With excess Grignard reagent, a nitrile and an aldehyde were cleanly converted to the amine and alcohol, respectively, and these moieties did not interfere with nickel catalyst: cyclopropane **4** was generated in good yields.

Next, we targeted additives with functional groups that can react with or serve as ligands for nickel catalysts (Figure 1). Aryl and alkyl chlorides did not outcompete the propargyl sulfonamide; the substituted vinylcyclopropane was observed in good yield. Alkenes strongly ligate nickel catalysts, so we evaluated two alkenes: cyclohexene and styrene. Cyclohexene was well-tolerated and did not inhibit the reaction, however, styrene inhibited the domino reaction likely due to strong ligation to the active catalyst. Finally, we evaluated nitrogen-containing heterocycles, common ligands for transition metals. In the presence of pyridine and a substituted pyridine the yield of cyclopropane **4** was lowered. Interestingly, when pyridine

was the additive, (*Z*)-alkene **4** was the major product.¹⁸ Indole and *N*-methyl indole did not affect the yields of the domino transformation. Finally, *N*-methylmorpholine inhibited the domino reaction resulting in diminished yield of cyclopropane **4**. Taken together, numerous functional groups are tolerated under our reaction conditions providing a robust domino reaction.

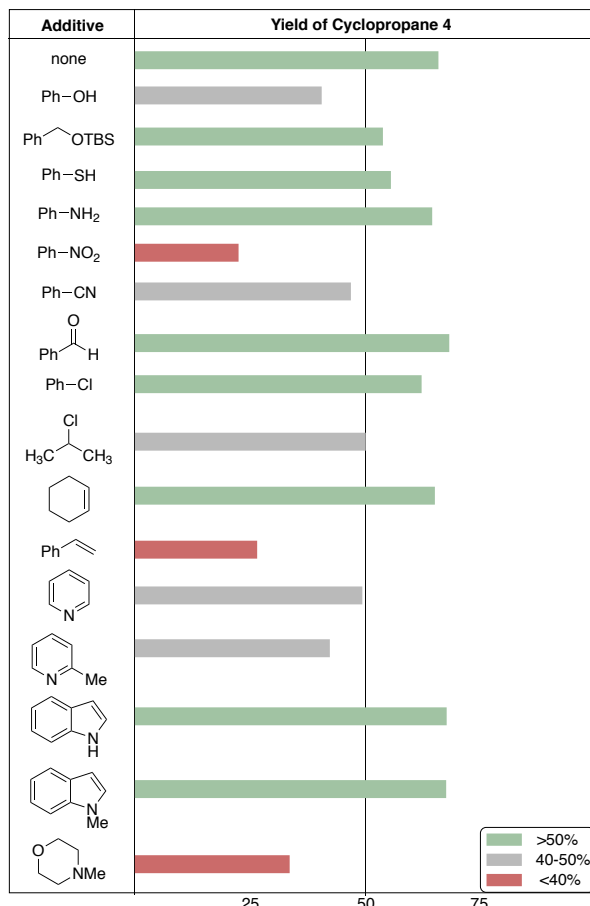
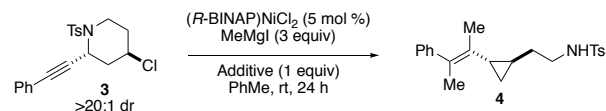
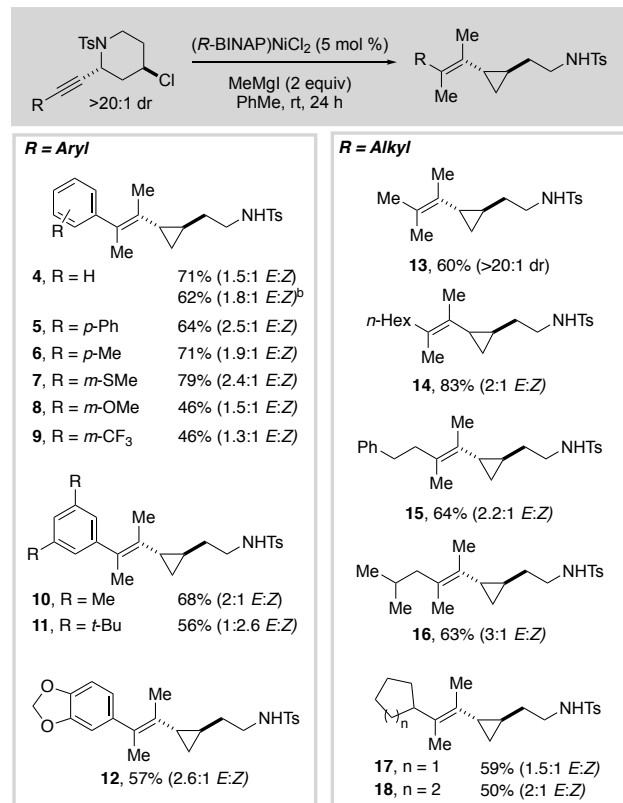


Figure 1. Robustness screen to establish functional group compatibility. (a) Yield of cyclopropane **4** determined by ¹H NMR based on comparison to PhTMS as an internal standard. (b) Unless otherwise noted, products were observed as ~1.5:1 mixture of (*E*)- and (*Z*)-alkene isomers. Employing pyridine and 2-methylpyridine as additives provided a slight preference for formation of the (*Z*)-alkene isomer (1:1.6 and 1:1.2 *E*:*Z* respectively).

Next, we evaluated the scope of the domino reaction (Scheme 2). Historically, cyclopropanes have been synthesized via Simmons–Smith reactions, transition metal-catalyzed carbene insertions, cycloisomerizations, and nucleophilic displacement reactions.³⁰ This method establishes an alternative to these strategies, while also providing a rapid synthesis of highly substituted vinylcyclopropanes.^{31, 32, 33} First, we evaluated substituted aromatic rings (**4–12**). We found that electron donating groups were well tolerated in the domino reaction, producing the desired product in excellent yields and moderate *E*:*Z* ratios. Interestingly, this reaction could be scaled up tenfold (to 1.0 mmol) and still retain good yield. The electron withdrawing CF₃ group provided the desired product albeit in moderate yield and diastereoselectivity. Interestingly, the

sterically bulky *t*-Bu substrate provided (*Z*)-alkene **11** as the major product. We hypothesize that the *t*-Bu groups hinder the carbometallation step and favor the intramolecular transmetalation leading to (*Z*)-vinylcyclopropane as the major product (*vide infra*). We were delighted to observe that aromatic groups were not necessary and alkyl substrates were able to undergo the transformation in excellent yields (**13–18**). It is important to note that cyclopropane **13** derived from propyne is obtained in excellent diastereoselectivity (>20:1) further confirming that cyclopropane formation is highly stereoselective.

Scheme 2. Substrate Scope^a

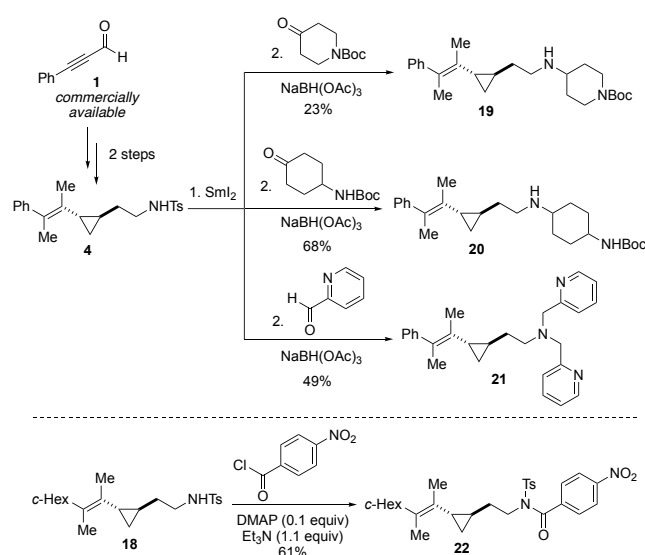


^aReactions performed on 0.1–0.2 mmol scale. Isolated yields.

^bReaction performed on 1.0 mmol scale.

Vinylcyclopropane and amine-substituted cyclopropane moieties are present in numerous biologically active compounds, natural products and pharmaceutical agents.^{34,35} For example, amino-substituted vinylcyclopropanes have been established as lysine specific demethylase (LSD1) inhibitors with potent anti-leukemia activity.³⁶ To demonstrate the synthetic potential of our domino reaction, we synthesized a series of analogs of LSD1 inhibitors (Scheme 3). First, we performed a SmI₂ deprotection of the pendant sulfonamide.³⁷ The resulting primary amine was subjected to three different reductive amination reactions to produce **19**, **20**, and **21**. Alternatively, the sulfonamide moiety could be functionalized directly via acylation to afford imide **22** in 61% yield. Interestingly, amine **20** demonstrated significant cell death against colon cancer cell lines (COLO-205 and HCC-2998) and imide **22** is active against a non-small cell lung cancer cell line (HOP-92).³⁸ Therefore, this domino reaction provides rapid access to bioactive structural motifs in four steps from commercially available materials.

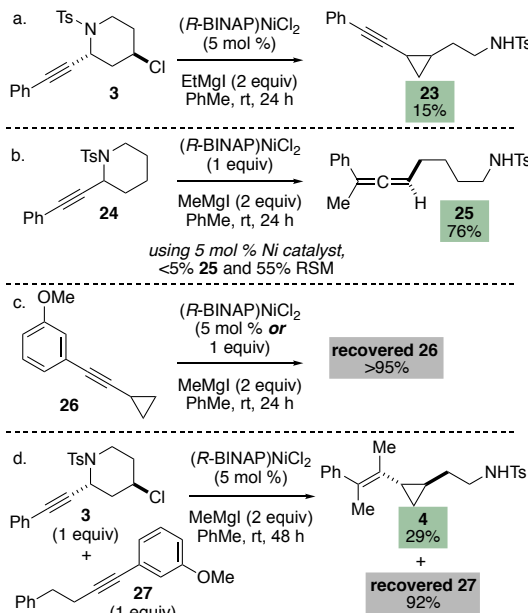
Scheme 3. Derivatization of Cyclopropane Products^{a,b,c}



^aSmI₂ (10 equiv), pyrrolidine (4 equiv), H₂O (5 equiv), rt, 5 min
^bNaBH(OAc)₃ (2 equiv), DCE, rt, 30 min. ^cYield over two steps.

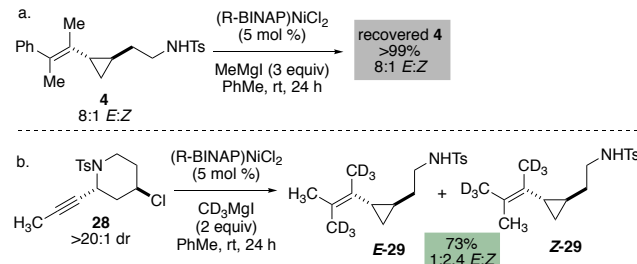
Next, we aimed to elucidate the mechanism of this multicomponent reaction. A series of control experiments were consistent with initiation of the catalytic cycle by oxidative addition of the nickel catalyst with the propargylic sulfonamide moiety. First, employing an alternative Grignard reagent, EtMgI, led to formation of alkynylcyclopropane **23** in 15% yield (Scheme 4a). This observation is consistent with oxidative addition of the propargylic sulfonamide to produce an allenylnickel complex that proceeds through an XEC pathway. A simple propargylic sulfonamide, **24**, lacking a pendant alkyl halide, underwent substitution to form allene **25**. This further supports that the mechanism initiates by oxidative addition of the propargylic sulfonamide. Additionally, simple alkynes did not undergo dicarbofunctionalization under standard reaction conditions (Scheme 4c and d). Alkynyl cyclopropane **26** did not undergo a 1,2-dicarbofunctionalization under standard reaction conditions, employing catalytic or stoichiometric quantities of nickel complex. Similarly, in a competition experiment, propargylic sulfonamide **3** reacted while alkyne **27** was not functionalized. Therefore, even in the presence of relevant catalytically active organonickel intermediates, a simple alkyne was not engaged. Taken together, these experiments support initiation of the domino reaction by oxidative addition of the propargylic sulfonamide moiety.

Scheme 4. Mechanistic Control Experiments



Next, we examined subsequent steps in the catalytic cycle, with a particular focus on the steps that would bifurcate to afford (*E*)- and (*Z*)-isomers of the alkene. To ensure that the product distribution was a kinetic distribution, we performed a control experiment (Scheme 5a). Resubjecting vinylcyclopropane **4** (8:1 *E*:*Z*) to the reaction conditions resulted in no isomerization. To determine whether the relative stability of product diastereomers is reflected in key transition states, we examined a substrate devoid of a steric preference for product formation (Scheme 5b). Employing a deuterated Grignard reagent provided vinylcyclopropane **29** as a 1:2.4 mixture (*E*:*Z*). Therefore, we concluded that the relative stability of product isomers does not impact the selectivity of the reaction.

Scheme 5. Kinetic and Thermodynamic Stability of Products



We next evaluated the reaction mechanism and origins of selectivity using density functional theory (DFT) calculations. The DFT-computed free energy changes of the catalytic cycle of (*Z*)-vinylcyclopropane **4** formation are shown in Figure 2. From the substrate-coordinated complex **INT1**, oxidative addition of the propargylic C–N bond can occur via **TS2** to generate the allenylnickel(II) intermediate **INT3**. This step is analogous to the S_N2-type oxidative addition mechanism identified in our previous mechanistic studies of Ni-catalyzed Kumada and XEC reactions of benzylic and allylic ethers and sulfonamides.^{9,10b} It also follows the known propensity of propargylic electrophiles to undergo oxidative addition with low-valent nickel complexes.³⁹ Additionally, consistent with our prior mechanistic studies,^{8c,9} the Lewis acid plays an important role in promoting oxidative addition. Lewis acidic

MgI_2 , present in solution due to Schlenk equilibrium of the Grignard reagent,⁴⁰ coordinates to the oxygen of the sulfonamide, which activates the substrate for oxidative

addition. The barrier for the same $\text{Ni}(0)$ -mediated oxidative addition increases by 14.6 kcal/mol without the assistance of MgI_2 (Figure S5).

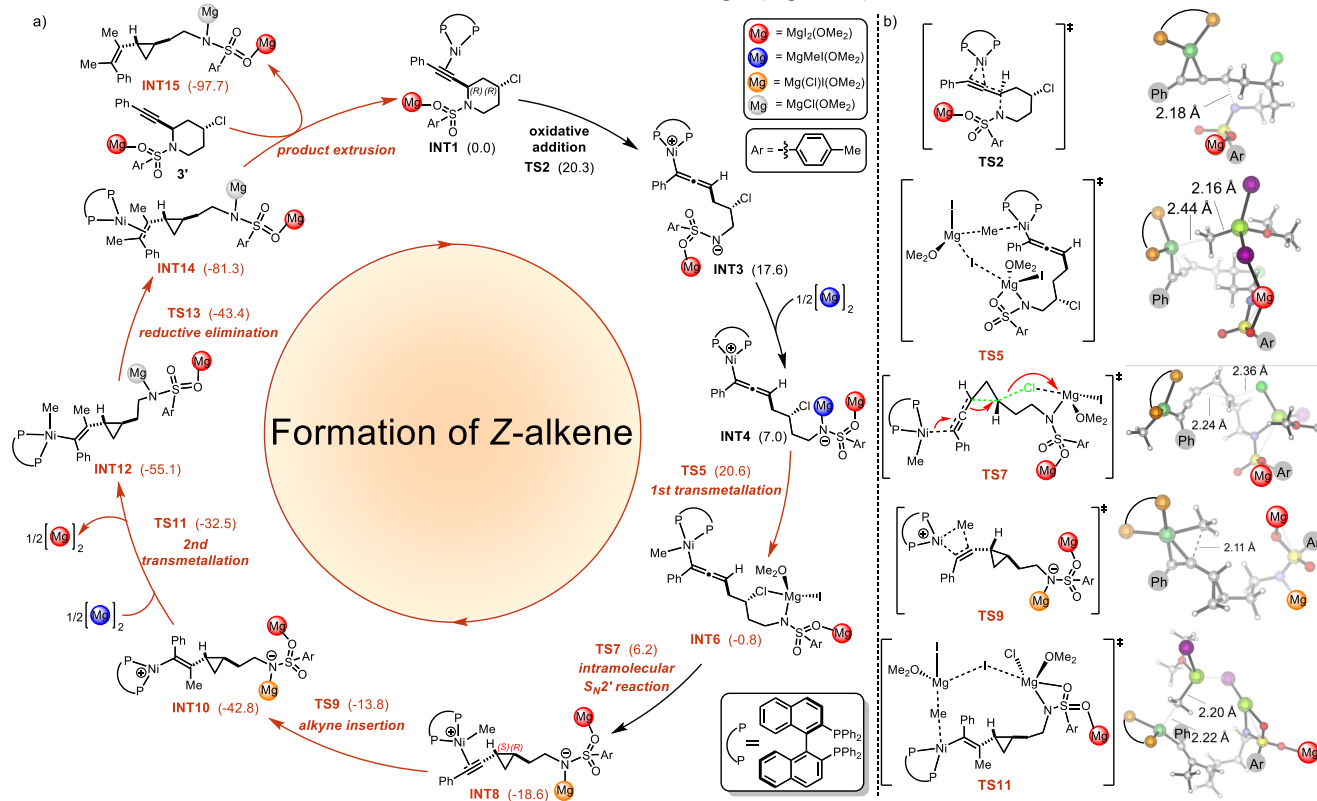


Figure 2. a) DFT-computed free energy changes of the catalytic cycle of nickel-catalyzed domino cross-electrophile coupling dicarbofunctionalization reaction for formation of (*Z*)-alkene, at the M06/def2-TZVPP-SMD(toluene)//B3LYP-D3(BJ)/def2-SVP-SMD(toluene) level of theory. b) Optimized structures of key transition states. All free energies are in kcal/mol.

After oxidative addition, allenynickel complex **INT3** cascades through the catalytic cycle. First, zwitterionic allenynickel(II) species **INT3** complexes with the Grignard reagent to afford intermediate **INT4**. Subsequent intramolecular transmetalation proceeds via **TS5** to generate the allenynickel(II) methyl intermediate **INT6**. This transmetalation increases the nucleophilicity of the allene moiety and allows the facile intramolecular $\text{S}_{\text{N}}2'$ -type reaction via **TS7** to produce the cyclopropane ring (**INT8**). We also considered the direct $\text{S}_{\text{N}}2'$ -type reaction of **INT4**, which is less favorable as compared to the transmetalation via **TS5** due to the poor nucleophilicity of the cationic allenynickel(II) moiety (Figure S6). From **INT8**, *syn*-migratory alkyne insertion of the methylnickel complex via **TS9** generates the (*Z*)-alkenynickel(II) intermediate **INT10**. Subsequent transmetalation and reductive elimination generates the alkene moiety as the (*Z*)-isomer. Final product extrusion liberates the (*Z*)-vinylcyclopropane product and regenerates the reactive intermediate **INT1** for the next catalytic cycle.

This mechanism could account for formation of the (*E*)-isomer of vinylcyclopropane product **4** if isomerization of the vinylnickel intermediate was feasible. Related isomerization reactions have been proposed to account for olefin isomers generated via vinylnickel species.⁴¹ However, calculated barriers demonstrate that the transmetalation of **INT10** is significantly faster than the *E*:*Z* isomerization to **INT17** (10.3 kcal/mol vs 15.7 kcal/mol, **TS11** vs. **TS16**, Figure 3). Therefore, the facile transmetalation of the cationic vinylnickel species prevents *E*:*Z* isomerization, and the catalytic cycle for

formation of (*Z*)-vinylcyclopropane formation does not account for the formation of (*E*)-vinylcyclopropane.

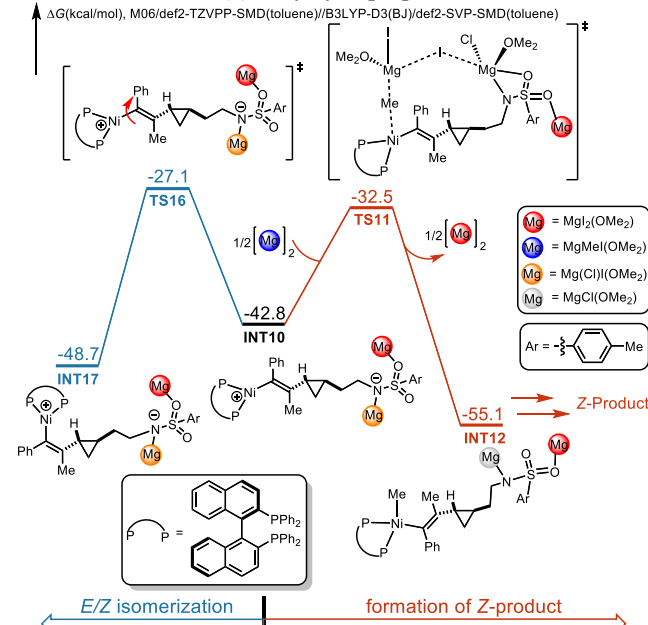


Figure 3. DFT-computed free energy barriers of the competing transmetalation and *E*:*Z*-isomerization of vinylnickel species.

The DFT-computed free energy profile of the (*E*)-vinylcyclopropane formation is shown in Figure 4. The catalytic cycle initiates with the same oxidative addition of the

propargylic sulfonamide to afford the zwitterionic allenylnickel(II) complex **INT3**, and this complex coordinates an equivalent of the Grignard reagent to afford **INT4**. At this point, the mechanism diverges. From **INT4**, instead of transmetallation which leads to (*Z*)-vinylcyclopropane, the

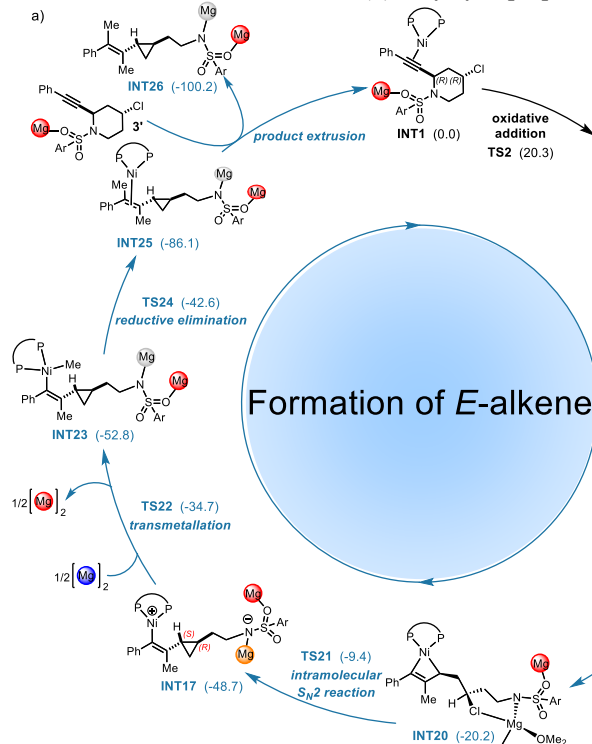
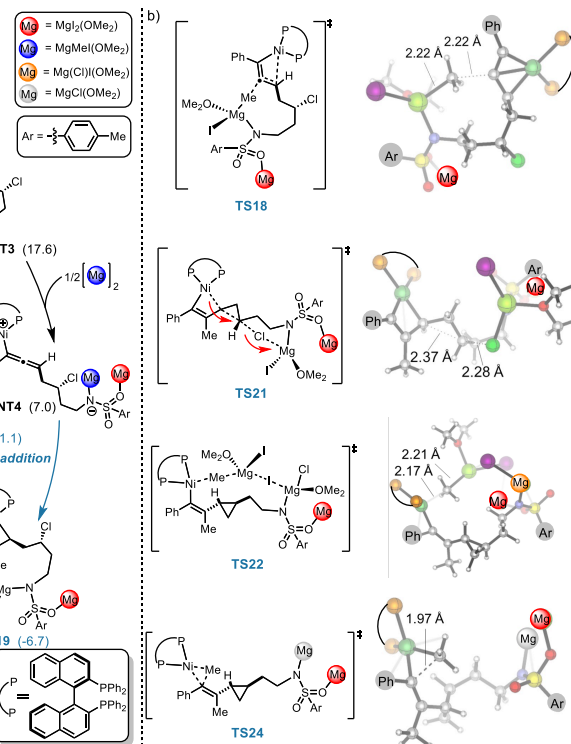


Figure 4. a) DFT-computed free energy changes of the catalytic cycle of nickel-catalyzed domino cross-electrophile coupling dicarbofunctionalization reaction for formation of (*E*)-alkene, at the M06/def2-TZVPP-SMD(toluene)//B3LYP-D3(BJ)/def2-SVP-SMD(toluene) level of theory. b) Optimized structures of key transition states. All free energies are in kcal/mol.

Subsequent steps in the catalytic cycle mirror those for formation of (*Z*)-vinylcyclopropane. Coordination of the alkyl halide to the tethered Grignard reagent provides **INT20**. A facile intramolecular S_N2 -type reaction via **TS21** generates the cyclopropane moiety of **INT17**. In **TS21**, the nucleophilic allylic position of the metallocyclobutene attacks the pendant alkyl chloride. In addition to generating the new C–C bond of the cyclopropane, this step provides a vinylnickel(II) moiety in **INT17**. Finally, transmetallation via **TS22** and subsequent C–C reductive elimination via **TS24** generates the tetrasubstituted olefin as the (*E*)-isomer. Product extrusion liberates the (*E*)-vinylcyclopropane product and regenerates the reactive intermediate **INT1**.

Based on the DFT-computed free energy profiles, the pathways for synthesis of (*Z*)- and (*E*)-vinylcyclopropane share the same oxidative addition step, and the chemoselectivity is determined by the competing transformations of zwitterionic allenylnickel(II) intermediate **INT4** (Figure 5). The classical transmetallation to nickel via **TS5** generates the $\text{LNi}(\text{allenyl})(\text{methyl})$ intermediate **INT6**, which irreversibly undergoes subsequent transformations to produce the (*Z*)-vinylcyclopropane product. The alternative carbometallation involves the attack of the internal carbon of the allene with the Grignard reagent. This step leads to the nickellacyclobutene intermediate **INT19** and eventually produces the (*E*)-vinylcyclopropane product. The *E*:*Z*-selectivity is determined by the competition between **TS5** and **TS18**, which only have a 0.5 kcal/mol free energy difference. This competition is

Grignard reagent can attack the internal carbon of the allenylnickel moiety to generate nickellacyclobutene **INT19**. This anti carbometallation reaction occurs via **TS18**. Similar nucleophilic additions to the internal carbon of an allene have been identified in related transformations.⁴²



consistent with the observed low *E*:*Z*-selectivity of the vinylcyclopropane formation.

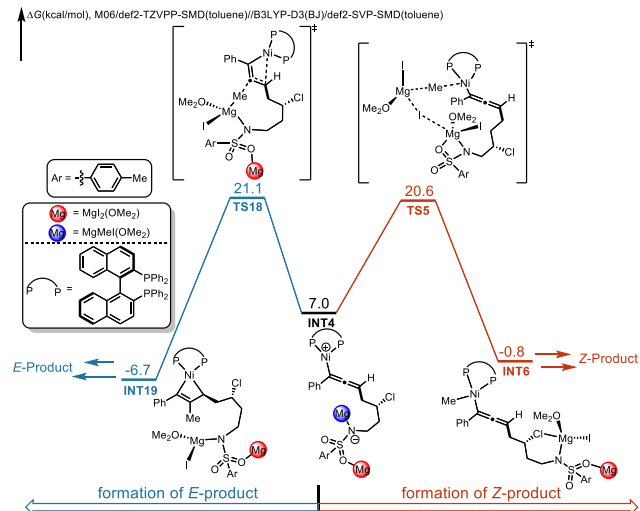
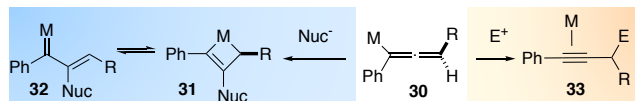


Figure 5. Mechanistic pathways that are responsible for the *E*:*Z*-selectivity.

Interestingly, this proposed bifurcated mechanism is consistent with the known ambiphilic reactivity of allenylmetal intermediates (Scheme 6).⁴² Nucleophiles tend to add to the central carbon, leading to formation of metallocyclobutene intermediates **31**. These metallocyclobutenes can equilibrate with vinylcarbene complexes **32**. In contrast, electrophiles tend to add to the terminal carbon. In our system, allenylmetal

complex **INT4** reacts with coordinated nucleophilic Grignard reagent to form metallocyclobutene **INT19**. However, if transmetallation proceeds, the resultant electron-rich allenylnickel moiety of **INT6** quickly attacks the pendant electrophilic alkyl chloride.



Scheme 6. Ambiphilic Pathways for Allenylmetal Species

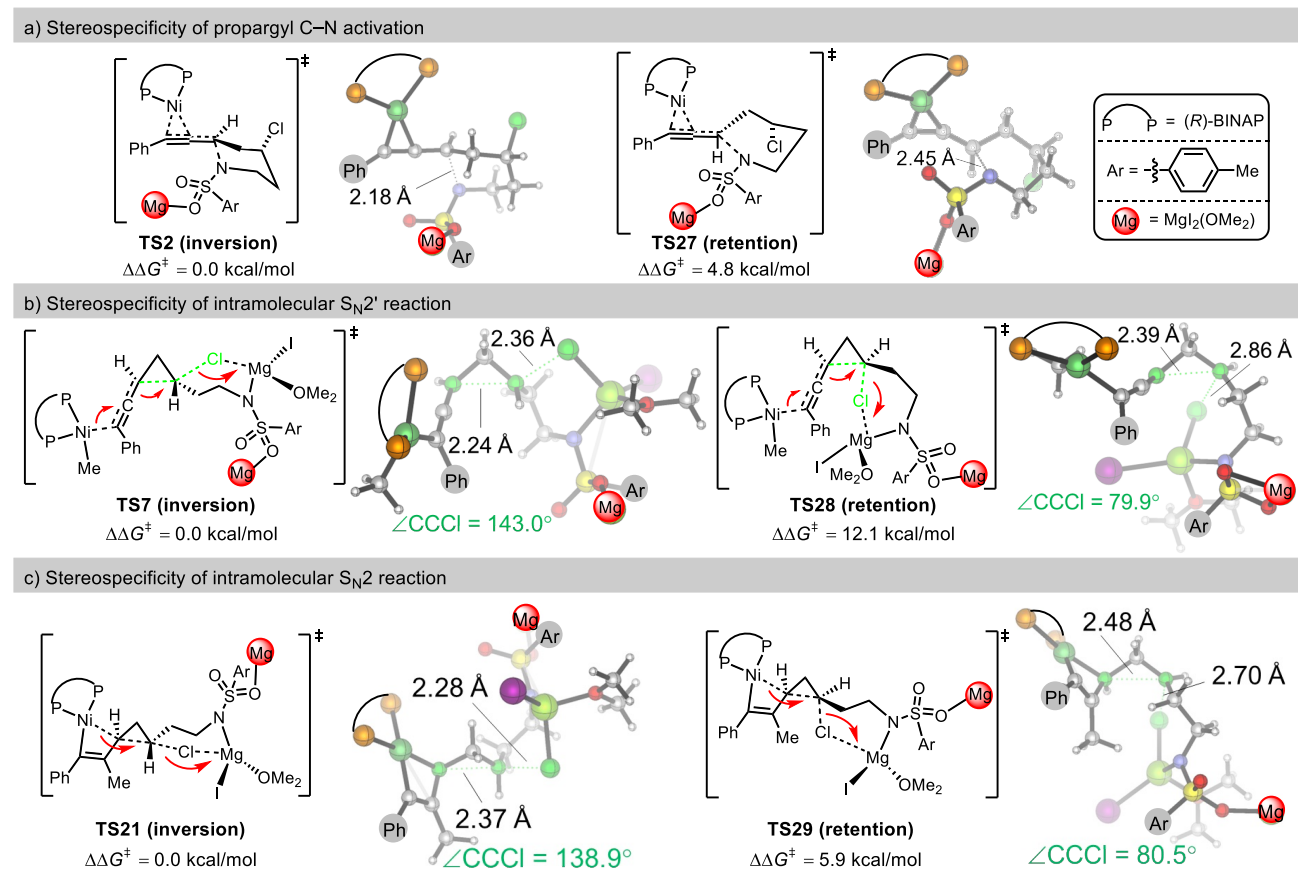


Figure 6. a) DFT-optimized structures and relative free energies of stereospecific propargyl C–N oxidative addition transition states. b) DFT-optimized structures and relative free energies of stereospecific intramolecular $\text{S}_{\text{N}}2'$ -type reaction transition states in (Z) -vinylcyclopropane formation. c) DFT-optimized structures and relative free energies of stereospecific intramolecular $\text{S}_{\text{N}}2$ -type reaction transition states in (E) -vinylcyclopropane formation.

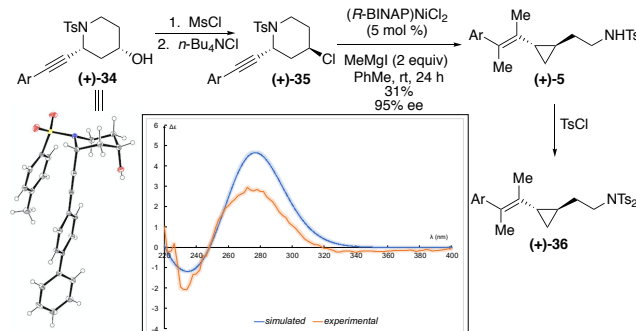
Based on the operative mechanistic pathway, we next examined the origins of stereoselectivity in formation of the cyclopropane moiety (Figure 6). The overall stereochemical outcome is determined by the oxidative addition of the propargylic C–N bond and the intramolecular $\text{S}_{\text{N}}2$ -type reaction for the formation of the cyclopropane. Oxidative addition can produce either stereoinversion or stereoretention, generating diastereomeric allenylnickel complexes.^{43, 44, 45} Our IRC calculations determined that oxidative addition is stereospecific and proceeds with inversion (Figure S7). The stereoinvertive transition state **TS2** is 4.8 kcal/mol more favorable than the stereoretentive transition state **TS27**, indicating an exclusively stereoinvertive propargylic oxidative addition. The intramolecular $\text{S}_{\text{N}}2$ -type reaction that generates the cyclopropane moiety also contributes to the stereochemical outcome of the reaction. This process exists in both the (Z) - and (E) -vinylcyclopropane formations, although the nature of the nucleophilic organonickel moiety differs. Both of the

intramolecular $\text{S}_{\text{N}}2$ -type reactions proceed exclusively with inversion at the alkynickel and alkylchloride positions and are strikingly similar despite the change of the alkylmetal moiety (**TS7** vs. **TS28**, **TS21** vs. **TS29**, Figure 6b, 6c). These exclusive stereoinvertive cyclopropanations follow the classic back-side $\text{S}_{\text{N}}2$ attack.⁹ The retentive cyclopropanations places the attacking nucleophile and the dissociating electrophile at the same face, which results in poor orbital overlap and is intrinsically disfavored.⁴⁶

Consistent with these computational results, we have confirmed experimentally that the cyclopropane ring formation is enantiospecific and occurs with retention (double inversion) at the sulfonamide-bearing carbon, and inversion at the alkyl chloride (Scheme 7). Enantioenriched alkynylpiperidine **34** was prepared by lipase-catalyzed kinetic resolution.⁴⁷ Absolute configuration of the starting material was assigned based on X-ray crystallographic analysis of alcohol **34**, a precursor of piperidine **35**. The absolute configuration of vinylcyclopropane

5 was determined by comparing the experimental circular dichroism spectrum to the simulated spectrum of imide 36.⁴⁸

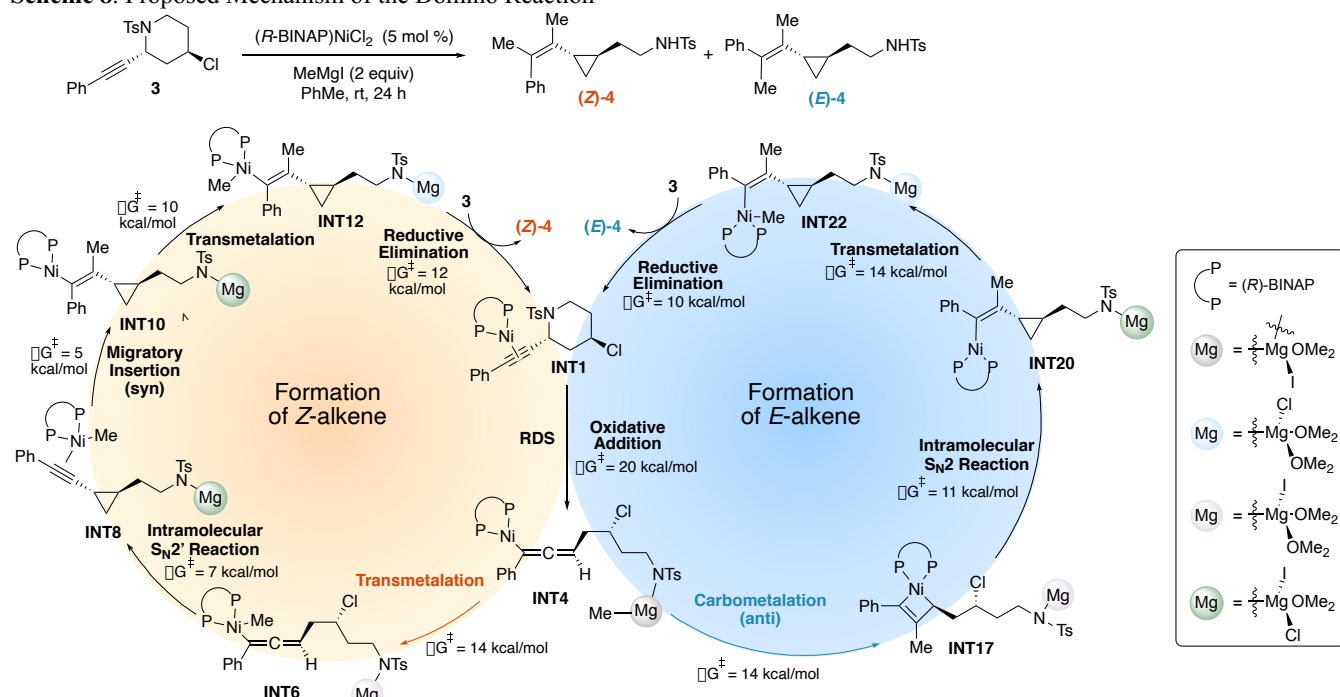
Scheme 7. Stereochemical Outcome of Domino Reaction.^{a,b,c}



^a MsCl (1.5 equiv), DMAP (0.1 equiv), Et₃N (1.5 equiv) DCM, rt, 2 h. ^b *n*-Bu₄NCl (2.0 equiv), THF, reflux 48 h. ^c TsCl (1.5 equiv), NaH (2 equiv), DMF, rt, 24 h.

Based on the experimental and computational mechanistic experiments, we propose the following domino mechanism (simplified version depicted in Scheme 8).⁹ Initiation of the catalytic cycle occurs with oxidative addition of the progargylic sulfonamide. The key allenylnickel intermediate **INT4** can react via two pathways. Carbometallation by nucleophilic attack of the pendant organomagnesium complex affords metallacyclobutene **INT17**, and eventually leads to formation of the major diastereomer, (*E*)-**4**. Alternatively, allenylnickel complex **INT4** can undergo transmetalation and subsequently attack the pendant electrophilic alkyl chloride, leading to formation of the minor diastereomer, (*Z*)-**4**. The pathways that diverge from allenylnickel intermediate **INT4** have transition states that are similar in energy, consistent with the observed modest levels of diastereoselectivity. Each elementary step is stereospecific, with *anti*-carbometallation and *syn*-reductive elimination providing (*E*)-**4** and *syn*-migratory insertion and *syn*-reductive elimination generating (*Z*)-**4**.

Scheme 8. Proposed Mechanism of the Domino Reaction



In conclusion, we report a nickel-catalyzed domino reaction, to the best of our knowledge, the first example that includes separate XEC and dicarbofunctionalization reactions. The net transformation consists of ring-contraction of the piperidine and dicarbomethylation of the alkyne, generating highly substituted cyclopropanes bearing tetrasubstituted olefins and aminoethyl substituents. The reaction products are structurally related to histone demethylase inhibitors and we report the synthesis of derivatives that demonstrate selective inhibition of colon and non-small cell lung cancer cell lines. In addition, to accomplish rapid synthesis of the requisite starting materials, we report the first aza-Prins reaction of simple ynals to afford alkynyl piperidines, the starting materials for this domino reaction. Experimental and computational analysis of the reaction mechanism support a bifurcated reaction mechanism that accounts for product distributions. After oxidative addition, a key allenylnickel intermediate partitions into two different pathways, each with similar barrier heights, that lead to the observed reaction

products. Future studies will include the development of related domino reactions and transformations that employ ambiphilic allenylnickel complexes.

ASSOCIATED CONTENT

Supporting Information

The Supporting Information is available free of charge on the ACS Publications website. Experimental details, NMR spectra, experimental and calculated circular dichroism spectra, computational details, energies, and Cartesian coordinates of calculated structures (link PDF)

AUTHOR INFORMATION

Corresponding Author

* E-mail: erjarvo@uci.edu.

* E-mail: hxchem@zju.edu.cn.

ORCID

Kirsten A. Hewitt: 0000-0002-9111-9837
Pei-Pei Xie: 0000-0002-7801-5232
Taylor A. Thane: 0000-0003-1271-1478
Nadia Hirbawi: 0000-0002-5759-3893
Shuo-Qing Zhang: 0000-0002-7617-3042
Alissa C. Matus: 0000-0002-4243-7089
Erika L. Lucas: 0000-0003-0714-3517
Xin Hong: 0000-0003-4717-2814
Elizabeth R. Jarvo: 0000-0002-2818-4038

Present Addresses

†If an author's address is different than the one given in the affiliation line, this information may be included here.

Author Contributions

‡These authors contributed equally.

¹ For reviews of transition-metal catalyzed domino reactions see: (a) Tietze, L. F. Domino Reactions in Organic Chemistry. *Chem. Rev.* **1996**, *96*, 115–136. (b) Ikeda, S.-I. Nickel-Catalyzed Intermolecular Domino Reactions. *Acc. Chem. Res.* **2000**, *33*, 511–519. (c) Montgomery, J. Nickel-Catalyzed Reductive Cyclizations and Couplings. *Angew. Chem. Int. Ed.* **2004**, *43*, 3890–3908. (d) Nicolaou, K. C.; Edmonds, D. J.; Bulger, P. G. Cascade Reactions in Total Synthesis. *Angew. Chem. Int. Ed.* **2006**, *45*, 7134–7186. (e) Pellissier, H. Stereocontrolled Domino Reactions. *Chem. Rev.* **2013**, *113*, 442–524. (f) Tietze, L. F. *Domino Reactions: Concepts for Efficient Organic Synthesis*. Wiley-VCH: Weinheim, **2014**.

² For reviews of XEC reactions see: (a) Knappke, C. E. I.; Grupe, S.; Gärtner, D.; Corpet, M.; Gosmini, C.; Jacobi von Wangelin, A. Reductive Cross-Coupling Reactions between Two Electrophiles. *Chem. Eur. J.* **2014**, *20*, 6828–6842. (b) Goldfogel, M. J.; Huang, L.; Weix, D. J. Cross-Electrophile Coupling: Principles and New Reactions. In *Nickel Catalysis in Organic Synthesis*; Ogoshi, S., Ed.; Wiley, **2020**; pp 183–222. (c) Wang, X.; Dai, Y.; Gong, H. Nickel-Catalyzed Reductive Couplings. *Top. Curr. Chem. (Z)* **2016**, *374*, 61–89. (d) Lucas, E. L.; Jarvo, E. R. Stereospecific and Stereoconvergent Cross-Couplings between Alkyl Electrophiles. *Nat. Rev. Chem.* **2017**, *1*, 0065. (e) Poremba, K. E.; Dibrell, S. E.; Reisman, S. E. Nickel-Catalyzed Enantioselective Reductive Cross-Coupling Reactions. *ACS Catal.* **2020**, *10*, 8237–8246. (f) Campeau, L.-C.; Hazari, N. Cross-Coupling and Related Reactions: Connecting Past Successes to the Development of New Reactions for the Future. *Organometallics* **2019**, *38*, 3–35.

³ For recent reviews of conjunctive XEC reactions see: (a) Qi, X.; Diao, T. Nickel-Catalyzed Dicarbofunctionalization of Alkene. *ACS Catal.* **2020**, *10*, 8542–8556. (b) Derosa, J.; Apolinar, O.; Kang, T.; Tran, V. T.; Engle, K. M. Recent Developments in Nickel-Catalyzed Intermolecular

ACKNOWLEDGMENT

This work was supported by the National Science Foundation (NSF) (CHE-1900340, E.R.J.), the National Natural Science Foundation of China (21702182 and 21873081, X. H.), Fundamental Research Funds for the Central Universities (2020XZZX002-02, X. H.), the State Key Laboratory of Clean Energy Utilization (ZJUCEU2020007, X. H.), the Center of Chemistry for Frontier Technologies, Department of Chemistry, Zhejiang University, and the Brython–Davis Fellowship (UCI, T.A.T.). We gratefully acknowledge Dr. Dima Fishman and the UC Irvine Laser Spectroscopy Laboratories for assistance in obtaining circular dichroism spectra. Dr. Felix Grun and the UC Irvine Mass Spectrometry Facility are acknowledged for mass spectrometry data. Dr. Joseph Ziller, UC Irvine X-ray Crystallographic Facility, is acknowledged for X-ray crystallographic data.

REFERENCES

Dicarbofunctionalization of Alkenes. *Chem. Sci.* **2020**, *11*, 4287–4296.

⁴ For recent reviews on nickel-catalyzed conjunctive XC reactions see: (a) Derosa, J.; Tran, V. T.; van der Puyl, V. A.; Engle, K. M. Carbon–Carbon π -Bonds as Conjunctive Reagents in Cross-Coupling *Aldrichimica ACTA* **2018**, *51*, 21–32. (b) Dhungana, R. K.; KC, S.; Basnet, P.; Giri, R. Transition Metal-Catalyzed Dicarbofunctionalization of Unactivated Olefins. *Chem. Rec.* **2018**, *18*, 1314–1340. (c) Luo, Y.-C. Xu, C.; Zhang, X. Nickel-Catalyzed Dicarbofunctionalization of Alkenes. *Chin. J. Chem.* **2020**, *38*, 1371–1394. For lead examples with alkynes: (d) Terao, H.; Bando, F.; Kambe, N. Ni-Catalyzed Regioselective Three-Component Coupling of Alkyl-Halides, Arylalkynes or enynes with R–M (M = MgX⁺, ZnX²⁺). *Chem. Commun.* **2009**, 7336–7338. (e) Xue, F.; Zho, J.; Hor, T. S. A.; Hayashi, T. Nickel-Catalyzed Three-Component Domino Reactions of Aryl Grignard Reagents, Alkynes, and Aryl Halides Producing Tetrasubstituted Alkenes. *J. Am. Chem. Soc.* **2015**, *137*, 3189–3192. (f) Wickham, L. M.; Giri, R. Transition Metal (Ni, Cu, Pd)-Catalyzed Alkene Dicarbofunctionalization Reactions. *Acc. Chem. Res.* **2021**, Article ASAP. DOI: [10.1021/acs.accounts.1c00329](https://doi.org/10.1021/acs.accounts.1c00329) (accessed 2021-8-17).

⁵ For lead examples of three-component conjunctive XEC reactions of alkenes see: (a) García-Domínguez, A.; Li, Z.; Nevado, C. Nickel-Catalyzed Reductive Dicarbofunctionalization of Alkenes. *J. Am. Chem. Soc.* **2017**, *139*, 6835–6838. (b) Shu, W.; García-Domínguez, A.; Quirós, M. T.; Mondal, R.; Cárdenas, D. J.; Nevado, C. Ni-Catalyzed Reductive Dicarbofunctionalization of Nonactivated Alkenes: Scope and Mechanistic Insights. *J. Am. Chem. Soc.* **2019**, *141*, 13812–13821. (c) Anthony, D.; Lin, Q.; Baudet, J.; Diao, T. Nickel-Catalyzed Asymmetric Reductive Diarylation of Vinylarenes. *Angew. Chem. Int. Ed.* **2019**, *58*, 3198–3202. (d) Wei, X.; Shu, W.; García-Domínguez, A.; Merino, E.; Nevado C. Asymmetric Ni-Catalyzed Radical

Relayed Reductive Coupling. *J. Am. Chem. Soc.* **2020**, *142*, 13515–13522. (e) Anthony, D.; Diao, T. Asymmetric Reductive Dicarbofunctionalization of Alkenes via Nickel Catalysis. *Synlett* **2020**, *31*, 1443–1447. (f) García-Domínguez, A.; Li, Z.; Nevado, C. Transforming Olefins into Dinucleophiles. *Chimia* **2018**, *72*, 212–215. (g) Zhao, X.; Tu, H.-Y.; Guo, L.; Zhu, S.; Qing, F.-L.; Chu, L. Intermolecular Selective Carboacylation of Alkenes via Nickel-Catalyzed Reductive Radical Relay. *Nat. Commun.* **2018**, *9*, 3488. (h) Yang, T.; Chen, X.; Rao, W.; Koh, M. J. Broadly Applicable Directed Catalytic Reductive Difunctionalization of Alkenyl Carbonyl Compounds. *Chem.* **2020**, *6*, 738–751. (i) Tu, H.-T.; Wang, F.; Huo, L.; Li, Y.; Zhu, S.; Zhao, X.; Li, H.; Qing, F.-L.; Chu, L. Enantioselective Three-Component Fluoroalkylarylation of Unactivated Olefins through Nickel-Catalyzed Cross-Electrophile Coupling. *J. Am. Chem. Soc.* **2020**, *142*, 9604–9611.

⁶ For selected lead examples of two component conjunctive XEC reactions of alkenes see: (a) Yan, C.-S.; Peng, Y.; Xu, X.-B.; Wang, Y.-W. Nickel-Mediated Inter- and Intramolecular Reductive Cross-Coupling of Unactivated Alkyl Bromides and Aryl Iodides at Room Temperature. *Chem. Eur. J.* **2012**, *18*, 6039–6048. (b) Xiao, J.; Wang, Y.-W.; Peng, Y. Nickel-Promoted Reductive Cyclization Cascade: A Short Synthesis of a New Aromatic Strigolactone Analogue. *Synthesis* **2017**, *49*, 3576–3581. (c) Kuang, Y.; Wang, X.; Anthony, D.; Diao, T. Ni-Catalyzed Two-Component Reductive Dicarbofunctionalization of Alkenes via Radical Cyclization. *Chem. Commun.* **2018**, *54*, 2558. (d) Wang, K.; Ding, Z.; Zhou, Z.; Kong, W. Ni-Catalyzed Enantioselective Reductive Diarylation of Activated Alkenes by Domino Cyclization/Cross-Coupling. *J. Am. Chem. Soc.* **2018**, *140*, 12364–12368. (e) Jin, Y.; Wang, C. Nickel-Catalyzed Asymmetric Reductive Arylalkylation of Unactivated Alkenes. *Angew. Chem. Int. Ed.* **2019**, *58*, 6722–6726. (f) Xu, S.; Wang, K.; Kong, W. Ni-Catalyzed Reductive Arylacylation of Alkenes toward Carbonyl Containing Oxindoles. *Org. Lett.* **2019**, *21*, 7498–7503. (g) Tian, Z.-X.; Qiao, J.-B.; Xu, G.-L.; Pang, X.; Qi, L.; Ma, W.-Y.; Zhao, Z.-Z.; Duan, J.; Du, Y.-F.; Su, P.; Liu, X.-Y.; Shu, X.-Z. Highly Enantioselective Cross-Electrophile Aryl-Alkenylation of Unactivated Alkenes. *J. Am. Chem. Soc.* **2019**, *141*, 7637–7643.

⁷ For a recent review of the mechanisms of inter- and intramolecular conjunctive XEC reactions see: (a) Diccianni, J.; Lin, Q.; Diao, T. Mechanisms of Nickel-Catalyzed Coupling Reactions and Applications to Alkene Functionalization. *Acc. Chem. Res.* **2020**, *53*, 906–919. (b) Lin, Q.; Diao, T. Mechanism of Ni-Catalyzed Reductive 1,2-Dicarbofunctionalization of Alkenes. *J. Am. Chem. Soc.* **2019**, *141*, 17937–17948.

⁸ (a) Tollefson, E. J.; Erickson, L. W.; Jarvo, E. R. Stereospecific Intramolecular Reductive Cross-Electrophile Coupling Reactions for Cyclopropane Synthesis. *J. Am. Chem. Soc.* **2015**, *137*, 9760–9763. (b) Erickson, L. W.; Lucas, E. L.; Tollefson, E. J.; Jarvo, E. R. Nickel-Catalyzed Cross-Electrophile Coupling of Alkyl Fluorides: Stereospecific Synthesis of Vinylcyclopropanes. *J. Am. Chem. Soc.* **2016**,

138, 14006–14011. (c) Lucas, E. L.; Hewitt, K. A.; Chen, P.-P.; Castro, A. J.; Hong, X.; Jarvo, E. R. Engaging Sulfonamides: Intramolecular Cross-Electrophile Coupling Reaction of Sulfonamides with Alkyl Chlorides. *J. Org. Chem.* **2020**, *85*, 1775–1793.

⁹ Chen, P.-P.; Lucas, E. L.; Greene, M. A.; Zhang, S.-Q.; Tollefson, E. J.; Erickson, L. W.; Taylor, B. L. H.; Jarvo, E. R.; Hong, X. A Unified Explanation for Chemoselectivity and Stereospecificity of Ni-Catalyzed Kumada and Cross-Electrophile Coupling Reactions of Benzylic Ethers: A Combined Computational and Experimental Study. *J. Am. Chem. Soc.* **2019**, *141*, 5835–5855.

¹⁰ (a) Tollefson, E. J.; Hanna, L. E.; Jarvo, E. R. Stereospecific Nickel-Catalyzed Cross-Coupling Reactions of Benzylic Ethers and Esters. *Acc. Chem. Res.* **2015**, *48*, 2344–2353. (b) Zhang, S.-Q.; Hong, X. Mechanism and Selectivity Control in Ni- and Pd-Catalyzed Cross Couplings Involving Carbon–Oxygen Bond Activation. *Acc. Chem. Res.* **2021**, *54*, 2158–2171.

¹¹ For reviews of nickel catalysis, see: (a) *Modern Organick Nickel Chemistry*; Tamari, Y., Ed.; Wiley-VCH: Weinheim; 2005. (b) Tasker, S. Z.; Standley, E. A.; Jamison, T. F. Recent Advances in Homogeneous Nickel Catalysis. *Nature* **2014**, *509*, 299–309. (c) *Nickel Catalysis in Organic Synthesis: Methods and Reactions*; Ogoshi, S., Ed.; Wiley, **2020**.

¹² Dicarbofunctionalization of alkynes with two equivalents of Grignard reagents have been reported: Dong, C.-G.; Yeung, P.; Hu, Q.-S. Two Palladium-Catalyzed Domino Reactions from One Set of Substrates/Reagents: Efficient Synthesis of Substituted Indenes and cis-Stilbenoid Hydrocarbons from the Same Internal Alkynes and Hindered Grignard Reagents. *Org. Lett.* **2007**, *9*, 363–366.

¹³ For an example of a nickel-catalyzed domino reaction that builds on XEC reactivity, see: Ping, Y.; Wang, K.; Pan, Q.; Ding, Z.; Zhou, Z.; Guo, Y.; Jong, W. Ni-Catalyzed Regio- and Enantioselective Domino Reductive Cyclization: One-Pot Synthesis of 2,3-Fused Cyclopentannulated Indoles. *ACS Catal.* **2019**, *9*, 7335–7342.

¹⁴ For reviews of the Prins/aza-Prins reaction see (a) Arundale, E.; Mikeska, L. A. The Olefin-Aldehyde Condensation. The Prins Reaction. *Chem. Rev.* **1952**, *51*, 505–555. (b) Adams, D. R.; Bhatnagar, S. P. The Prins Reaction. *Synthesis*, **1977**, 661–672. (c) Olier, C.; Kaafarani, M.; Gastaldi, S.; Bertrand, M. P. Synthesis of Tetrahydropyrans and Related Heterocycles via Prins Cyclization: Extension to Aza-Prins Cyclization. *Tetrahedron*, **2010**, *66*, 413–445. (d) Pastor, I. M.; Yus, M. Focused Update on the Prins Reaction and the Prins Cyclization. *Curr. Org. Chem.* **2012**, *16*, 1277–1312. (e) Reddy, B. V. S.; Nair, P. N.; Antony, A.; Lalli, C.; Grée, R. The Aza-Prins Reaction in the Synthesis of Natural Products and Analogues. *Eur. J. Org. Chem.* **2017**, 1805–1819.

¹⁵ Olier, C.; Gastaldi, S.; Gil, G.; Bertrand, M. P. Protected Propargylic Acetals. Nicholas-Prins Cyclization leading to Functionalized 2-alkynyl-tetrahydropyrans. Intramolecular Trapping by Allenes. *Tetrahedron Lett.* **2007**, *48*, 7801–7804.

¹⁶ (a) Osawa, C.; Tateyama, M.; Miura, K.; Tayama, E.; Iwamoto, H.; Hasegawa, E. An Effective Procedure to Promote Aza-Prins Cyclization Reaction Employing a Combination of Ferric Chloride and an Imidazolium Salt in Benzotrifluoride. *Heterocycles* **2012**, *86*, 1211–1226. (b) ref 8c

¹⁷ (a) Zhang, H.; Muñiz, K. Selective Piperidine Synthesis Exploiting Iodine-Catalyzed Csp^3 –H Amination under Visible Light. *ACS Catal.* **2017**, *7*, 4122–4125. (b) Seel, S.; Thaler, T.; Takatsu, K.; Zhang, C.; Zippe, H.; Straub, B. F.; Mayer, P.; Knochel, P. Highly Diastereoselective Arylations of Substituted Piperidines. *J. Am. Chem. Soc.* **2011**, *133*, 4774–4777.

¹⁸ See Supporting Information for details

¹⁹ For lead references of XEC of ammonium salts, aziridines, and pyridinium salts, see: (a) Moragas, T.; Gaydou, M.; Martin, R. Nickel-Catalyzed Carboxylation of Benzylic C–N Bonds with CO_2 . *Angew. Chem., Int. Ed.* **2016**, *55*, 5053–5057. (b) Woods, B. P.; Orlandi, M.; Huang, C.-Y.; Sigman, M. H.; Doyle, A. G. Nickel-Catalyzed Enantioselective Reductive Cross-Coupling of Styrenyl Aziridines. *J. Am. Chem. Soc.* **2017**, *139*, 5688–5691. (c) Liao, J.; Basch, C. H.; Hoerrner, M. E.; Talley, M. R.; Boscoe, B. P.; Tucker, J. W.; Garnsey, M. R.; Watson, M. P. Deaminative Reductive Cross-Electrophile Couplings of Alkylpyridinium Salts and Aryl Bromides. *Org. Lett.* **2019**, *21*, 2941–2946. (d) Wang, J.; Hoerner, M. E.; Watson, M. P.; Weix, D. J. Nickel-Catalyzed Synthesis of Dialkyl Ketones from the Coupling of *N*-alkyl Pyridinium Salts with Activated Carboxylic Acids. *Angew. Chem. Int. Ed.* **2020**, *59*, 13484–13489. For reviews on the activation of C–N bonds see: (e) Ouyang, K.; Hao, W.; Zhang, W.-X.; Xi, Z. Transition-Metal-Catalyzed Cleavage of C–N Single Bonds. *Chem. Rev.* **2015**, *115*, 12045–12090. (f) Wang, Q.; Su, Y.; Li, L.; Huang, H. Transition-Metal Catalyzed C–N Bond Activation. *Chem. Soc. Rev.* **2016**, *45*, 1257–1272.

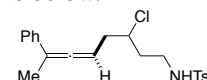
²⁰ For synthesis of (*R*-BINAP)NiCl₂, see: (a) Standley, E. A.; Smith, S. J.; Muller, P.; Jamison, T. F. A Broadly Applicable Strategy for Entry into Homogenous Nickel(0) Catalysts from Air-Stable Nickel(II) Complexes. *Organometallics* **2014**, *33*, 2012–2018. (b) Dawson, D. D.; Oswald, V. F.; Borovik, A. S.; Jarvo, E. R. Identification of the Active Catalyst for Nickel-Catalyzed Stereospecific Kumada Coupling Reactions of Ethers. *Chem. Eur. J.* **2020**, *26*, 3044–3048.

²¹ Fluoride leaving groups were evaluated due to the success of the XEC Reactions of vinyl tetrahydropyrans. See ref 8b for further information.

²² (a) Greene, M. A.; Yonova, I. M.; Williams, F. J.; Jarvo, E. R. Traceless Directing Group for Stereospecific Nickel-Catalyzed Alkyl–Alkyl Cross-Coupling Reactions. *Org. Lett.* **2012**, *14*, 4293–4296. (b) Felkin, H.; Swierczewski, G. Stereochemical Evidence in Favour of π -allylnickel Intermediates in the Formation of Olefins from Allylic Alcohols and Grignard Reagents, Catalysed by Nickel Complexes. *Tetrahedron Lett.* **1972**, *13*, 1433–1436.

²³ Tran, V. T.; Li, Z.-Q.; Apolinar, O.; Derosa, J.; Joannou, M. V.; Wisniewski, S. R.; Eastgate, M. D.; Engle, K. M. Ni(COD)(DQ): An Air-Stable 18-Electron Nickel(0)-Olefin Precatalyst. *Angew. Chem. Int. Ed.* **2020**, *59*, 7409–7413.

²⁴ See supporting information for further details. The structure of the product is below.



²⁵ For examples of propargylic displacement by Grignard reagents, see: (a) Gore, J.; Dulcere, J. P. New Synthesis of Vinylallenenes. *J. Chem. Soc., Chem. Commun.* **1972**, 866–867. (b) Krause, N.; Hoffmann-Röder, A. Synthesis of Allenes with Organometallic Reagents. *Tetrahedron* **2004**, *60*, 11671–11694.

²⁶ Copper catalysts are also known to promote propargyl substitution reactions. (a) Zhang, D.-E.; Hu, X.-P. Recent Advances in Copper-Catalyzed Propargylic Substitution. *Tetrahedron Lett.* **2015**, *56*, 283–295. (b) Roy, R.; Saha, S. Scope and Advances in the Catalytic Propargylic Substitution Reaction. *RSC. Adv.* **2018**, *8*, 31129–31193. (c) Miyake, Y.; Uemura, S.; Nishibayashi, Y. Catalytic Propargylic Substitution Reactions. *ChemCatChem* **2009**, *1*, 342–356.

²⁷ For copper-catalyzed reactions with propargylic ammonium salts see: (a) Guisán-Ceinos, M.; Martín-Heras, V.; Soler-Yanes, R.; Cárdenas, D. J.; Tortosa, M. Copper-Catalysed Cross-Coupling of Alkyl Grignard Reagents and Propargylic Ammonium Salts: Stereospecific Synthesis of Allenes. *Chem. Commun.* **2018**, *54*, 8343–8346. (b) Guisán-Ceinos, M.; Martín-Heras, V.; Tortosa, M. Regio- and Stereospecific Copper-Catalyzed Substitution Reaction of Propargylic Ammonium Salts with Aryl Grignard Reagents. *J. Am. Chem. Soc.* **2017**, *139*, 8448–8451.

²⁸ Copper catalysts are known to promote dicarbofunctionalization reactions. For representative examples see: (a) You, W.; Brown, M. K. Diarylation of Alkenes by a Cu-Catalyzed Migratory Insertion/Cross-Coupling Cascade. *J. Am. Chem. Soc.* **2014**, *136*, 14730–14733. (b) You, W.; Brown, M. K. Catalytic Enantioselective Diarylation of Alkenes. *J. Am. Chem. Soc.* **2015**, *137*, 14578–14581. (c) Thapa, S.; Basnet, P.; Giri, R. Copper-Catalyzed Dicarbofunctionalization of Unactivated Olefins by Tandem Cyclization/Cross-Coupling. *J. Am. Chem. Soc.* **2017**, *139*, 5700–5703.

²⁹ Collins, K.; Glorius, F. A Robustness Screen for the Rapid Assessment of Chemical Reactions. *Nature Chem.* **2013**, *5*, 597–601.

³⁰ For reviews on the synthesis of vinylcyclopropanes see: (a) Lebel, H.; Marcoux, J.-F.; Molinaro, C.; Charette, A. B. Stereoselective Cyclopropanation Reactions. *Chem. Rev.* **2003**, *103*, 977–1050. (b) Bartoli, G.; Bencivenni, G.; Dalpozzo, R. Asymmetric Cyclopropanation Strategies. *Synthesis*, **2014**, *46*, 979–1029. (c) Ebner, C.; Carreira, E. M. Cyclopropanation Strategies in Recent Total Syntheses. *Chem. Rev.* **2017**, *117*, 11651–11679; (d) Wu, W.; Lin, Z.; Jiang, H. Recent Advances in the Synthesis of Cyclopropanes. *Org. Biomol. Chem.* **2018**, *16*, 7315–7329. (e) Mato, M.; Franchino, A.; García-Morales, C.; Echavarren, A. M. Gold-Catalyzed Synthesis of Small Rings. *Chem. Rev.* **2021**, *121*, 8613–8684.

³¹ For selected cross-coupling approaches for the synthesis of vinylcyclopropanes, see (a) Charette, A. B.; Giroux, A. Palladium-Catalyzed Suzuki-Type Cross-Couplings of Iodocyclopropanes with Boronic Acids: Synthesis of *trans*-1,2-Dicyclopentyl Alkenes. *J. Org. Chem.* **1996**, *61*, 8718–8719. (b) Yao, M.-L.; Deng, M.-Z. Palladium-Catalyzed Cross-Coupling of Cyclopropylboronic Acids with Alkenyl Triflates. *Tetrahedron Lett.* **2000**, *41*, 9083–9087. (c) Hu, L.; Shen, P.-X.; Shao, Q.; Hong, K.; Qiao, J.; Yu, J.-Q. Pd^{II}-Catalyzed Enantioselective C(sp³)-H Activation/Cross-Coupling Reactions of Free Carboxylic Acids. *Angew. Chem. Int. Ed.* **2018**, *58*, 2134–2138.

³² For transformations of vinylcyclopropanes, see: (a) Jiao, L.; Yu, Z.-X. Vinylcyclopropane Derivatives in Transition-Metal-Catalyzed Cycloadditions for the Synthesis of Carbocyclic Compounds. *J. Org. Chem.* **2013**, *78*, 6842–6848. (b) Rubin, M.; Rubina, M.; Gevorgyan, V. Transition-Metal Chemistry of Cyclopropenes and Cyclopropanes. *Chem. Rev.* **2007**, *107*, 3117–3179. (d) Souillart, L.; Cramer, N. Catalytic C–C Bond Activation via Oxidation Addition to Transition Metals. *Chem. Rev.* **2015**, *115*, 9410–9464. (e) Wang, J.; Blaszczyk, S. A.; Li, X.; Tang, W. Transition Metal-Catalyzed Selective Carbon–Carbon Bond Cleavage of Vinylcyclopropanes in Cycloaddition Reactions. *Chem. Rev.* **2020**, *121*, 110–139.

³³ For Fe-catalyzed conjunctive XC reactions of vinylcyclopropanes that proceeds with ring-opening, see: (f) Liu, L.; Lee, W.; Yuan, M.; Acha, C.; Geherty, M. B.; Williams, B.; Guterrez, O. Intra- and Intermolecular Fe-Catalyzed Dicarbofunctionalization of Vinyl Cyclopropanes. *Chem. Sci.* **2020**, *11*, 3146–3151.

³⁴ For reviews on biological activity of substituted vinyl cyclopropanes, see: (a) Talele, T. T. The “Cyclopropyl Fragment” is a Versatile Player that Frequently Appears in Pre-clinical/Clinical Drug Molecules. *J. Med. Chem.* **2016**, *59*, 8712–8756. (b) Salaün, J. Cyclopropane Derivatives and their Diverse Biological Profile. In *Small Ring Compounds in Organic Synthesis VI*. de Meijere, A. Ed. **2000**. pp. 1–67.

³⁵ For discussions on the biological activity of substituted alkenes, see: (a) Avendano, C.; Menendez, J. C. *Medicinal Chemistry of Anticancer Drugs*, Elsevier, Oxford, **2015**, pp. 87–95. (b) Flynn, A. B.; Ogilvie, W. W. Stereocontrolled Synthesis of Tetrasubstituted Olefins. *Chem. Rev.* **2007**, *107*, 4698–4745.

³⁶ Albrecht, B. K.; Audia, J. E.; Cote, A.; Duplessis, M.; Gehling, V. S.; Harmange, J.-C.; Vaswani, R. G. LSD1 Inhibitors and Uses Thereof. WO 2016/172496 A1. 2016.

³⁷ (a) Szostak, M.; Spain, M.; Procter, D. J. Preparation of Samarium (II) Iodide: Quantitative Evaluation of the Effect of Water, Oxygen, and Peroxide Content, Preparative Methods, and the Activation of Samarium Metal. *J. Org. Chem.* **2012**, *77*, 3049–3059. (b) Ankner, T.; Hilmersson, G. Instantaneous Deprotection of Tosylamides and Esters with SmI₂/Amine/H₂O. *Org. Lett.* **2009**, *11*, 503–506.

³⁸ (a) Shoemaker, R. H. The NC160 Human Tumour Cell Line Anticancer Drug Screen. *Nat. Rev. Cancer* **2006**, *6*, 813–823. (b) National Institute of Health, “National Cancer Institute Developmental Therapeutics Program,” can be found under <https://dtp.cancer.gov/>, 2021.

³⁹ (a) Arzoumanian, H.; Cochini, F.; Nuel, D.; Petrignani, J. F.; Rosas, N. Mono- and Dicarboxylation of α -Haloalkynes by Nickel Cyanide under Phase-Transfer Conditions. *Organometallics* **1992**, *11*, 493–495. (b) Arzoumanian, H.; Cochini, F.; Nuel, D.; Petrignani, J. F.; Rosas, N. Nickel- and Phase-Transfer-Catalyzed Carboxylation of Propargyl and Allenyl Halides. *Organometallics* **1993**, *12*, 1871–1875. (c) Li, Q.-H.; Liao, J.-W.; Huang, Y.-L.; Chiang, R.-T.; Gau, H.-M. Nickel-Catalyzed Substitution Reactions of Propargyl Halides with Organotitanium Reagents. *Org. Biomol. Chem.* **2014**, *12*, 7634–7642. (d) Shao, X. B.; Zhang, Z.; Li, Q. H. Zhao, Z. G. Synthesis of Multi-Substituted Allenes from Organoalane Reagents and Propargyl Esters by Using a Nickel Catalyst. *Org. Biomol. Chem.* **2018**, *16*, 4797–4806.

⁴⁰ (a) Schlenk, W.; Schlenk, W. Jr. Über die Konstitution der Grignardschen Magnesiumverbindungen. *Ber. Dtsch. Chem. Ges. B* **1929**, *62*, 920–924. (b) Wurtz, A. Sur une nouvelle classe de radicaux organiques. *Ann. Chim. Phys.* **1855**, *44*, 275. (c) Wurtz, A. Ueber eine neue Klasse organischer Radicale. *Justus Liebigs Ann. Chem.* **1855**, *96*, 364.

⁴¹ For vinylnickel isomerizations: (a) Huggins, J. M.; Bergman, R. G. Mechanism, Regiochemistry, and Stereochemistry of the Insertion Reaction of Alkynes with Methyl(2,4-pentaedionato)(triphenylphosphine)nick-el. A Cis Insertion that Leads to Trans Kinetic Products. *J. Am. Chem. Soc.* **1981**, *103*, 3002–3011. (b) Hernández, J.; Müller, G.; Rocamora, M.; Solans, X.; Auilgó, M. Reactions of Activated Alkynes with Organonickel Complexes. Crystal Structure of Trans-[NiBr(C(COOMe)=C(COOMe)(3,5-Cl₂C₆H₃))(PPh₃)₂]. *J. Organomet. Chem.* **1988**, *345*, 383–396.

⁴² (a) Minami, I.; Yuhara, M.; Watanabe, H.; Tsuji, J. A New Furan Annelation Reaction by the Palladium-Catalyzed Reaction of 2-Alkynyl Carbonates or 2-(1-alkynyl)oxiranes with β -keto esters. *J. Organomet. Chem.* **1987**, *334*, 225–242. (b) Casey, C. P.; Nash, J. R.; Yi, C. S.; Selmeczy, A. D.; Chung, S.; Powell, D. R.; Hayashi, R. K. Kinetic Addition of Nucleophiles to η^3 -Propargyl Rhenium Complexes Occurs at the Central Carbon to Produce Rhenacyclobutenes. *J. Am. Chem. Soc.* **1998**, *120*, 722–733. (c) Chen, J.-T. Addition Reactions of Mononuclear η^3 -Allenyl/Propargyl Transition Metal Complexes: A New Class of Potent Organometallic Carbon Electrophiles. *Coord. Chem. Rev.* **1999**, *190*–*192*, 1143–1168. (d) Tsuji, J.; Mandai, T. Palladium-Catalyzed Reactions of Propargylic Compounds in Organic Synthesis. *Angew. Chem. Int. Ed. Engl.* **1995**, *34*, 2589–2612. (e) Ma, S. Pd-Catalyzed Coupling Reactions Involving Propargylic/Allenylidic Species. *Eur. J. Org. Chem.* **2004**, *6*, 1175–1183. (f) Cheng, Y.-C.; Chen, Y.-K.; Huang, T.-M.; Yu, C.-I.; Lee, G.-H.; Wang, Y.; Chen, J.-T. Synthesis of Metallacyclobutenes of Late Transition Metals via Nucleophilic Addition of Allenyl or Propargyl Complexes. *Organometallics* **1998**, *17*, 2953–2957. (g) Holland, R. L.; Bunker, K. D.; Chen, C. H.; DiPasquale, A. G.; Rheingold, A. L.; Baldridge, K. K.; O'Connor, J. M. Reactions of a Metallacyclobutene Complex with Alkenes. *J. Am. Chem. Soc.* **2008**, *130*, 10093–10095.

⁴³ For stereospecific transformations of propargylic ethers with copper complexes, see: (a) Marek, I.; Mangeney, P.; Alexakis, A.; Normant, J. F. Are Allenes Formed from Propargylic Ethers through a Syn or Anti Displacement? *Tetrahedron Lett.* **1986**, *27*, 5499–5502. (b) Alexakis, A.; Marek, I.; Mangeney, P.; Normant, J. F. Mechanistic Aspects of the Formation of Chiral Allenes from Propargylic Ethers and Organocopper Reagents. *J. Am. Chem. Soc.* **1990**, *112*, 8042–8047.

⁴⁴ For nickel-catalyzed stereoablative reactions of propargylic electrophiles, see: (a) Smith, S. W.; Fu, G. C. Nickel-

Catalyzed Asymmetric Cross-Couplings of Racemic Propargylic Halides with Arylzinc Reagents. *J. Am. Chem. Soc.* **2008**, *130*, 12645–12647. (b) Oelke, A. J.; Sun, J.; Fu, G. C. Nickel-Catalyzed Enantioselective Cross-Couplings of Racemic Secondary Electrophiles That Bear an Oxygen Leaving Group. *J. Am. Chem. Soc.* **2012**, *134*, 2966–2969.

⁴⁵ Kinetic studies and DFT calculations have been carried out for the oxidative addition of propargyl halides with a dimethylplatinum (II) complex: Hoseini, S. J.; Nasrabadi, H.; Fath, R. H.; Moradi, Z.; Rashidi, M. Oxidative Addition of Propargyl Halides, Chloroacetonitrile, and Ethyl Chloroacetate to a Dimethylplatinum(II) Complex: Kinetic and DFT Studies. *Organometallics* **2014**, *33*, 1689–1699.

⁴⁶ (a) Anh, N. T.; Minot, C. Conditions Favoring Retention of Configuration in S_N2 Reactions. A Perturbational Study. *J. Am. Chem. Soc.* **1980**, *102*, 103–107. (b) Glukhovtsev, M. N.; Pross, A.; Schlegel, H. B.; Bach, R. D.; Radom, L. Gas-Phase Identity S_N2 Reactions of Halide Anions and Methyl Halides with Retention of Configuration. *J. Am. Chem. Soc.* **1996**, *118*, 11258–11264.

⁴⁷ CCDC 2104034. See Supporting Information for details. For lipase-catalyzed kinetic resolution of 4-hydroxytetrahydropyrans, see: Yadav, J. S.; Reddy, B. V. S.; Padmavani, B.; Venugopal, C.; Rao, A. B. Enzymatic Kinetic Resolution of Racemic 4-Tetrahydropyranols by *Candida Rugosa* Lipase. *Tetrahedron Lett.* **2007**, *48*, 4631–4633.

⁴⁸ Bannwarth, C.; Grimme, S. A Simplified Time-Dependent Density Functional Theory Approach for Electronic Ultraviolet and Circular Dichroism Spectra of Very Large Molecules. *Comput. Theor. Chem.* **2014**, *1040*–*1041*, 45–53.

TOC Graphic

